Res Chem Intermed (2017) 43:297–320
DOI 10.1007/s11164-016-2623-7

Evaluation of poly ε-caprolactone electrospun nanofibers loaded with *Hypericum perforatum* extract as a wound dressing

Faegheh Pourhojat[1] · Mahmoodreza Sohrabi[1] · Shahab Shariati[2] · Hamid Mahdavi[3] · Leila Asadpour[4]

Received: 16 April 2016 / Accepted: 22 June 2016 / Published online: 15 July 2016

Abstract In this study, for the first time, a biocompatible and non-toxic herbal wound dressing was made by encapsulation of *Hypericum perforatum* alcoholic extract at different concentrations (10, 30 and 50 % v/v) into poly ε-caprolactone electrospun nanofibers to achieve an effective wound dressing. The electrospinning processing parameters such as needle tip to collector distance, applied voltage and flow rate of feed solution were changed until accumulated nano-scale fibers without bead structures were obtained. Then, the morphology of the nanofibrous structures was investigated by scanning electron microscopy. After synthesis of the nanofibers in optimal conditions, the antibacterial activity of the optimized bandages was investigated by the disc diffusion method against strains of *Staphylococcus aureus* and *Escherichia coli*. The release content of the herbal drug was tested by the total immersion method in phosphate buffer saline and displayed a constant drug liberation with time. Water vapor transmission rate for the wound dressing was evaluated by pseudo-extra cellular fluid for optimal samples. The crystallinity and thermal behavior of the mats with and without *H. perforatum* alcoholic extract were studied by X-ray diffraction and differential scanning calorimetry. The results of antibacterial activity, cell culture and In vitro methyl thiazolyl tetrazolium assays demonstrated these unique structures as being very useful as burn and ulcer dressings.

✉ Mahmoodreza Sohrabi
Sohrabymahmoodreza@gmail.com

[1] Department of Chemistry, North Tehran Branch, Islamic Azad University, P.O. Box 1913674711, Tehran, Iran

[2] Department of Chemistry, Rasht Branch, Islamic Azad University, Rasht, Iran

[3] Iran Polymer and Petrochemical Institute Polymer Engineering, Tehran, Iran

[4] Department of Veterinary Science, Rasht Branch, Islamic Azad University, Rasht, Iran

Keywords *Hypericum perforatum* · Poly ε-caprolactone · Electrospinning · Nanofibers · Antibacterial activity

Introduction

Human skin acts as an anatomical barrier against pathogens but its proper structural performance can be impaired as a result of physical, chemical, thermal and surgery damage. Because of disruption in the normal connection of a tissue due to wounds, skin can lose its protective role and the accumulation of infection can bring undesirable consequences. Thus, in the spontaneous wound healing process by which the body itself overcomes the tissue damage, the cure rate is very slow and the risk of bacterial infection is high. Solving this problem requires a material to raise the healing rate. Wound healers are one of the most important prerequisites in the wound healing process. Herbal wound healers reduce the necessity of using synthetic drugs such as chemical antibiotics and avoids the side effects of using them [1–3].

The application of medicinal plants in wound and burn healing processes by ethnic tradition has been common for a long time. The most effective dressing should provide bacterial and mechanical protection, facilitate fluid and gas exchange, and should also be easily removed with the least damage to the skin thus reducing scarring and accelerating the wound healing by retaining moisture in moderation.

Due to the unique properties of nanofibrous dressings, such as high oxygen permeability, structural similarity to the extracellular matrix, high surface to volume ratio and tunable pore size, this category of wound dressings is very suitable [4–6]. Nanofibers do not have the problems such as accumulation and clustering related to nanoparticles and produce non-woven mats that even after wound healing remain relatively intact [7]. The small pore-ized membranes made by electrospinning prevents the penetration of bacteria and external microbial factors to the wound area, but oxygen easily passes through the holes of the matrix and reaches the wound, as a result causing no problem for skin breathing. Among the methods of production of nanofibers, electrospinning is one of the best methods due to its suitable price and the production of continuous fibers [8, 9].

The advantages of transdermal drug delivery systems are the reduction of drug dosing frequency due to the longer time of drug release, the uniform increase in blood plasma levels, reduced side effects, simple removal of covers from the wound, painlessness and compatibility with patient conditions.

Pit [10], as one of the pioneers in the characterization and description of the application of resorbable polymers including poly ε-caprolactone (PCL), has carried out several researches in this field including in vitro [11, 12] and in vivo studies [13].

Researches have also included the subcutaneous transfer of L-methadone from PCL microspheres [14]. Following this research, PCL was applied as a very thin film for covering skin wounds [15] and also as a release device for chlorohegzidin (a chemical disinfectant). Medicinal plants are good choices for wound healing due to their non-toxic features and high compatibility with physiologic and biologic conditions. For example, curcumin, the saponin extracted from turmeric, has both

anti-oxidant and anti-inflammatory effects. PCL electrospun nanofibrous mats containing curcumin were prepared by Merle et al. and were used in diabetic wound healing with the release of the drug for 72 h and with anti-oxidant activity suitable for oxygen radical absorbance [16–21]. The conclusion is that nanofibers loaded with curcumin caused a reduction in inflammation that showed an increased rate of wound closure in a diabetic mouse model. The use of *Centella asiatica* extract for burn wound healing and skin disorders has also been reported [17, 22]. In a similar study, wound dressing fiber systems containing *Biophytum sensitivum*, which is an important medicinal plant in traditional medicine in Asia, Africa and the Pacific, were used. Beneficial effects of *Biophytum sensitivum* include anti-inflammatory, anti-infection, and diuretic antipyretic properties that have been studied in electrospun PCL fibers loaded with the drug thymol (the biggest component of thymol oil) [23]. The addition of thymol as an antibacterial agent and as a proliferation factor in electrospun nanofibrous polymeric mats as wound dressings has been reported by Karimi et al. [24].

According to our knowledge, there is no report indicating the addition of *Hypericum perforatum* as an anti-microbial agent in nanofibrous polymeric mats as a transdermal drug delivery system. PCL is a flexible polymer that has a good compatibility with other polymers and is mainly degraded by microbial agents. PCL is a bio-absorbative polymer that has been studied as a wound dressing material since 1970 [25]. *Hypericum perforatum* plant is a medicinal herb with a long history of wound healing due to the antimicrobial activity of crude extracts. Hypericum oil is used conventionally for rapid recovery of ulcers and burns because of its wound healing activity [26].

In this research, the chemical characterization of electrospun nanofibers was evaluated by different characterization methods and, by controlling the processing parameters, fibrous PCL scaffolds were obtained with controllable fiber diameters at the nano-scale. The morphology of the synthesized mats was studied by scanning electron microscopy (SEM) and the mats were characterized by Fourier transform infrared spectroscopy (FT-IR), differential scanning calorimetry (DSC) and X-ray diffraction (XRD). The release of *Hypericum perforatum* extracts from the PCL mats was studied with UV–Vis spectrophotometry.

Materials and methods

Materials

PCL (MW = 80,000 Da) was obtained from Sigma-Aldrich (Milwaukee, WI, USA). Dichloromethane (DCM), *N*,*N* dimethyl formamide (DMF) and Triton-X100 were supplied from Merck (Darmstadt, Germany). All materials were used directly without any further purification. *Hypericum perforatum* alcoholic extract was obtained from Zardband Pharmaceuticals (Tehran, Iran). The salts of NaCl, KCl, Na_2HPO_4, $NaHCO_3$, Na_2CO_3 and K_2HPO_4 were purchased from Merck. Muller Hinton Agar (MHA) was purchased from Merck. Bacterial strains containing *Staphylococcus aureus* (*S. aureus*) (PTCC1113) and *Escherichia coli* (*E. coli*)

(PTCC1399) were prepared from the Persian Type Culture Collection. Bacterial strains were grown in tryptic soy broth.

Preparation of electrospun nanofiber membranes

PCL fibrous membranes were prepared by electrospinning a PCL solution at a concentration of 7 % (w/v) in DCM:DMF [80:20 (v/v)]. PCL/*Hypericum perforatum* fibers with 10, 30 and 50 % (v/v) of alcoholic *Hypericum perforatum* extract were obtained by electrospinning their mixed solution in DCM:DMF (80:20, v/v). These solutions were prepared by dissolving the exact amount of PCL in DCM:DMF (80:20 v/v) as solvent. Then, the alcoholic extract of *Hypericum perforatum* was slowly added into the prepared polymer solution, while stirring vigorously for 1 h until complete dissolution. To obtain homogeneous solutions, Triton X-100 was used as a surfactant, while, to improve the electrospinning process, dibasic potassium phosphate salt was added. Electrospinning of PCL fibers was carried out at room temperature with an applied voltage of 10–25 kV (HV Power Supply; Gamma High Voltage Research, Ormond, Fanavaran Nano Meghyas, Tehran, Iran) and a plastic syringe with a blunt-tip stainless steel spinneret (15.8 mm diameter) kept at a distance of 100–200 mm from the fiber collector (a wood plate covered with aluminum sheet as a grounded electrode) was used. The needle of the syringe was connected to the positive high voltage. A manual syringe pump (SP1000; Fanavaran Nano Meghyas) was used to control the flow rate of the feed solution. Continuous PCL fibers were collected on the aluminum foil in the form of a non-woven fibrous mat. Electrospinning conditions were optimized to produce PCL nanofibrous mats composed of individual fibers without bead formation. In the following, fibers obtained by electrospinning will be described as PCL-E_n where n is the amount (worded as volumetric percentage) of *Hypericum perforatum* extract present.

Characterization

Quantification of total hypericin content in plant alcoholic extract

The total content of hypericin obtained from the *Hypericum perforatum* alcoholic extract was determined by spectrophotometric method and expressed in hypericin% (g/g) [27] The optical absorbance of the solution was read at a 587-nm wavelength, in a 1-cm quartz cell, compared to phosphate buffer saline (PBS) as a blank. The concentration of hypericin was evaluated by the aid of absorbance measured at 587 nm and using Eq. (1)

$$\text{Hyp}\,\% = \frac{A}{780}\frac{100}{m} \tag{1}$$

where A is the measured absorbance, m the grams of residual after drying of 25 ml of extract, and 780 the specific absorbance of hypericin at 587 nm.

To determine the content of hypericin in the sample, 25 ml of the extract was placed in an incubator at 37 °C. The dried extract was weighed after 2 weeks, and

then solutions with various dilutions of dried extract were prepared and the optical absorbance of each solution was read at 587 nm. Based on the obtained standard curve of the analyzed sample, the hypericin content was calculated according to Eq. (1).

Morphological study

The morphology of the electrospun nanofibers was characterized by scanning electron microscopy (SEM; JEOL JSM-T300, USA). A small section of the synthesized fiber mat was placed on the SEM sample holder and sputter-coated with gold prior to the analysis.

XRD measurements

The XRD measurements were carried out with a Bruker diffractometer (equipped with a continuous scan attachment and a proportional counter) using Ni-filtered Cu K_α radiation source ($\lambda = 1.54050$ Å), at 40 kV and 40 mA.

FT-IR spectroscopy

The FT-IR of the synthesized PCL nanofibers was carried out using a Nicolet™ iS™ 50 FT-IR spectrometer in the range of 500–4000 cm^{-1} to confirm the incorporation of herbal drug in the polymeric membranes.

Thermal analysis

DSC analysis of electrospun PCL and PCL-E_n nanofibrous mats was carried out with a thermal analysis (TA) instruments model 2010 (DuPont, USA) at a heating rate of 2 °C min^{-1}. Before DSC analysis, all the samples were kept in a desiccator with silica gel. Then, the electrospun samples were sealed in aluminum pans and heated from 0 to 200 °C. The empty pan was used as the reference. The degree of crystallinity (X_c) of the PCL in the nanofibrous membrane was calculated by the Eq. (2):

$$X_c(\%) = \Delta H_m / \Delta H_m^* \times 100\,\% \tag{2}$$

where ΔH_m^* is 142 J g^{-1}, which is the theoretical heat of fusion for 100 % crystalline PCL [28].

Water vapor transmission rate (WVTR) measurement

Preparation of pseudo extracellular fluid (PECF)

PECF which simulates the wound fluids, was prepared by dissolving 0.68 g of sodium chloride (NaCl), 0.22 g of potassium chloride (KCl), 2.5 g of sodium hydrogen carbonate ($NaHCO_3$) and 0.35 g of sodium dihydrogen phosphate

(NaH_2PO_4) in 100 ml of distilled water [29]. The pH of PECF was adjusted to 8 ± 0.2.

Measuring WVTR

The WVTR across the membranes was measured by utilizing a bottle with an exposure area of 1.76 cm^2 which was filled with 10 ml PECF and its opening was covered by a circular nanofibrous mat. The bottles were placed in an upright position inside an oven at 37 °C containing 1 kg of freshly dried silica gel to maintain relatively low humidity conditions. The weight of the assembly was measured every hour for 12 h and a graph of evaporated water versus time was plotted. WVTR was calculated using Eq. (3):

$$\mathrm{WVTR} = \frac{\mathrm{Slope} \times 24}{\mathrm{area}} \left[\frac{\mathrm{g}}{\mathrm{day\ m^2}}\right] \tag{3}$$

The data were reported as mean ± SD for five parallel runs [30].

PECF absorption

The capacity of PCL and PCL-E_n membranes to absorb wound exudates was determined by soaking the 1 × 1.5 cm^2 rectangular samples in PECF. They were first weighed and put in each well of a 24-well cell-culture plate filled with 2 ml PECF (pH = 8) and placed in an incubator at 37 °C. After 24 h, the samples were weighed immediately after being blotted with filter paper to remove excessive surface solution. The percentage of fluid absorption was calculated according to the following equation:

$$\text{Fluid absorption percentage} = \frac{W_{s-}W_o}{W_o} \times 100 \tag{4}$$

where W_s is the weight of the swollen sample and W_o is the initial dry samples weight. The data were reported as mean ± SD of three parallel runs [23].

Porosity determination

The porosity of the membranes was measured at room temperature using Eq. (5). In the dimensional approach, the density of the drug-loaded membranes was calculated from the exact dimensional values for each sample in air. The electrospun membranes were cut into 10-mm discs and weighted. The surface of the membranes and thickness of the samples were measured by a digital micrometer. The density of bulk PCL was taken as 1.145 g cm^{-3}

$$\text{Porosity} = (1 - \rho/\rho_o) \times 100\,\% \tag{5}$$

where ρ is the density of the electrospun membrane and ρ_o is the density of the bulk polymer [28].

In vitro drug release measurement

In vitro drug release from the synthesized nanofibers was studied by measuring the absorbance of hypericin at 587 nm using a UV–VIS spectrophotometer (model UV-2401; Shimadzu, Japan). The tests were performed using rectangular specimens of 5×5 cm^2 of the mats with a thickness of 30 μm, placed into 25 ml of PBS (pH = 7.4) and stirred at 100 rpm at 37 °C in an shaking incubator (model 211DS; Labnet International, USA). Next, 2 ml of release medium containing hypericin was withdrawn at fixed time intervals of 2, 8, 34 and up to 990 h (42 days), and replenished with fresh medium. Then, the absorbance of withdrawn sample at 587 nm was read and compared with the calibration curve. Meanwhile, the amount released from the nanofibers was calculated according to the following equation:

$$C'_n = C_n \left(\frac{V_T}{V_T - V_S} \right) \left(\frac{C'_{n-1}}{C_{n-1}} \right) \tag{6}$$

where C'_n is the corrected concentration of the nth sample, mg l^{-1}; C_n is the measured concentration of hypericin in the nth sample in mg l^{-1}; C_{n-1} is the measured concentration of the $n-1$th sample in mg l^{-1}; V_T is the volume of receiving fluid, ml; and V_S is the volume of withdrawn sample (2 ml) [31]. By considering the Eq. (6), the release percentage was calculated and reported.

In vitro study of antibacterial activity

The inhibitory action of the electrospun PCL-E$_n$ nanofibers with different concentrations of *Hypericum perforatum* extract was evaluated by the disc diffusion method according to the specifications of the document M2-A9 from the Clinical and Laboratory Standards Institute [32]. Aliquots of the cryogenic reserve of *S. aureus* and *E. coli* were inoculated in 7-ml Tryptic soy broth tubes. Each bacterium was adjusted to 0.5 Mcfarland in 0.9 % sodium chloride solution prior to their inoculation in Muller Himton Agar (MHA(plates. Three membranes in the shape of discs of 10 mm in diameter were sterilized under UV light for 2 h and placed onto MHA plates. The procedure was repeated three times for each bacterium. The plates were inverted face down and incubated at 37 °C for 24, 48 and 72 h. The activity against the bacteria was evaluated using the agar well diffusion method as described by Boyanova et al. and Kroiss et al. [33, 34]. A Vancomycin antibiogram disc, as a positive control, was placed onto one MHA plate and incubated under the same conditions.

Cell line and sub culturing

In the present study, human fibroblast normal cell lines were grown in order to evaluate the PCL-E$_n$ nanofibers cellular adhesion and proliferation. After sterilization of nanofibrous mats with an area of 1×1 cm^2 using gamma radiation, samples were put in 24-well plates, while, to evaluate the remaining solvent, nanofibrous mats were rinsed (3 times) using PBS solution.

Cells with a concentration of 5000 cell ml^{-1} well were cultured on the surface of the scaffold and were put on Dulbeco's Modified Eagle's medium (DMEM) containing 10 % fetal bovin serum (FBS), streptomycin 1 % and penicillin 1 % for 4 days, and maintained at 37 °C in a humified incubator containing 5 % CO_2. Then, for fixing, cells on the nanofibrous medium within the wells were removed and the well contents were rinsed using PBS solution and glutaraldehyde solution was put on the mats for 45 min [35], after which the mats were dehydrated by ethanol solution at a concentration of 35, 70, 75 and 96 % and the samples were fixed and dried for evaluation by SEM tests.

Determination of cell viability (MTT assay)

This study was carried out to valuate the cytotoxicity of neat PCL and PCL-E_{10} nanofibrous mats. For this purpose, the indirect method according to ISO 10993 standard was applied [36]. Nanofibrous mats were cut into 1 × 2 cm^2 pieces and, after sterilization by gamma radiation, were put into 24-well plated. Then, 2.5 ml of culture medium of DMEM without FBS was poured onto each sample and placed in an incubator for 1 and 5 days at 37 °C. Also, two wells containing culture medium without the sample as a control were incubated for 1 and 5 days. After this period, the call flask was tripsinized and centrifuged and then the fibroblast cells were counted and poured into each well of a 96-multiwell tissue culture plate at a density of 10,000 cells (10,000 cell ml^{-1} per well), and incubated with 100 ml of medium containing FBS for 24 h. Then, the cell culture medium was completely removed and, instead, 90 µl of the extract of nanofibrous mats prepared in 1 and 5 days was poured into cells, with 10 µl of FBS added to each well, and incubated for 24 h. After this period, the supernatant fluid was removed and, instead, 100 µl of MTT solution at a density of 0.5 mg ml^{-1} in PBS was poured into each well and incubated for 4 h. Then, wells containing MTT solution were emptied and, instead, 100 ml/well of DMSO was added to dissolve the formazan crystals. Finally, after shaking for 15 min in a shaker incubator, the absorbance was read by Elisa Reader (at $\lambda = 570$ nm). From each sample, 6 wells were filled with extract and the data obtained were averaged.

The biocompatibility percent of the samples was calculated by dividing the absorbance of wells containing extract with the absorbance of the control wells.

Results and discussion

Morphology and structure

In order to achieve a suitable solvent system which can uniformly prepare a polymer solution containing the plant extract, PCL pellets were dissolved in DCM:DMF (80:20) mixed solvent at ambient conditions with different concentrations of *Hypericum perforatum* alcoholic extract (10, 30 and 50 % v/v) after which, in spite of initial homogeneity, a two-phase system was formed over time. To solve this problem, Triton X-100 was used as a surfactant (3 % w/v), while to prepare uniform

defect-free nanofibers, K_2HPO_4 salt was used (0.78 % w/v). The morphologies of the electrospun PCL mats containing different concentrations of *Hypericum perforatum* alcoholic extract without salt are shown in Fig. 1. The SEM micrographs and the diameter distribution of the obtained fibrous membranes of PCL, PCL-E_{10}, PCL-E_{30} and PCL-E_{50} with salt are shown in Fig. 2.

There are many experimental parameters affecting fiber morphology. Some of these parameters are interrelated, and isolating the effect of each one is difficult. For this reason, typically, the one at a time approach has been employed based on changing the solution and the spinning parameters to obtain uniform mats. PCL-E_0, PCL-E_{10}, PCL-E_{30} and PCL-E_{50} solutions were electrospun under different experimental conditions and all the optimum experimental conditions for obtaining nanofiberous mats are reported in Table 1.

Regarding the effects of salts in increasing the conductivity of the polymeric solutions, using K_2HPO_4 salt resulted in the formation of free bead nanofibers. Also, effective process parameters in electrospinning, such as applied voltage, flow rate and nozzle to collector distance, were changed and optimal conditions were selected regarding SEM images to obtain nano-scale fibers.

The nanofibrous structure of the pristine PCL sample was characterized as individual, uniform, and randomly oriented fibers with an average diameter of 245 nm. The addition of *Hypericum perforatum* extract changed the diameter of nanofibers dramatically. The fiber dimension distributions were evaluated by ImageJ software which showed that fiber dimension distribution is slightly shifted towards higher dimensions centered near 400 nm after the addition of *Hypericum perforatum*. This increase in the fiber diameters and junctions may be due to the incorporation of the extract which reduces the solvent evaporation rate. When the solvent evaporation rate reduces, excess solvent may cause the fibers to merge where they are in contact to form junctions resulting in inter-and intra-layer bonding [37].

Quantification of total hypericin content in plant alcoholic extract

The content of hypericin in the alcoholic extract as one of the antibacterial agents available in herbal extract was determined by spectrophotometric method.

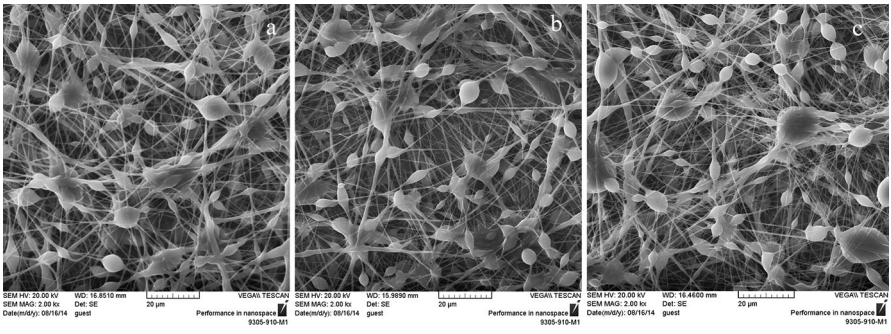

Fig. 1 SEM micrographs of PCL-E_{10} (**a**), PCL-E_{30} (**b**), PCL-E_{50} (**c**) without K_2HPo_4

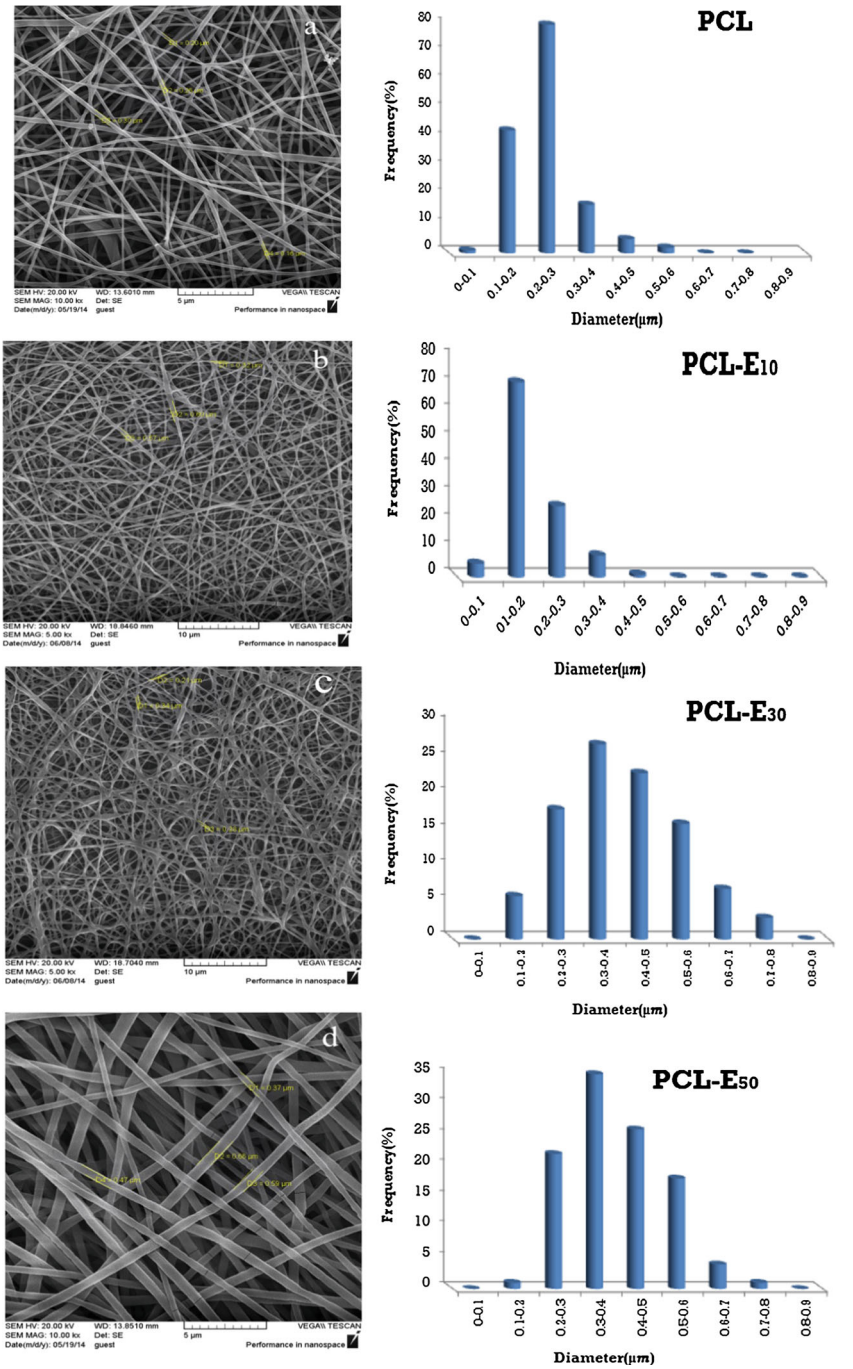

Fig. 2 SEM micrographs and diameter distribution of PCL (**a**), PCL-E_{10} (**b**), PCL-E_{30} (**c**), PCL-E_{50} (**d**)

Table 1 Fiber diameter, porosity and optimum conditions of electrospun PCL and PCL-E$_n$ nanofiber membranes

Samples	Average diameter (nm)	Diameter distribution (nm)	Porosity (%)	Experimental condition for obtaining optimal membranes		
				KV (V)	Distance (*D*) (cm)	Flow rate (ml/h)
Pure PCL	245	79–527	91.2	20	10	0.5
PCL-E$_{10}$	328	79–448	91.34	20	10	0.5
PCL-E$_{30}$	412	117–712	92.85	15	10	0.5
PCL-E$_{50}$	400	212–794	91	12	10	0.5

Table 2 The content of hypericin in dried extract (g % Hyp)

Sample	Dried extract (ppm)	Dried extract (g)	Absorbance in λ_{587}	Hyp $(g\%) = \frac{A_{587}}{\varepsilon bm} \times 100$
1	6000	0.3	0.477	0.2038
2	4000	0.2	0.341	0.2185
3	3000	0.15	0.2305	0.1970
4	1000	0.05	0.065	0.1666
5	500	0.025	0.031	0.1589
6	200	0.01	0.0185	0.237
7	100	0.005	0.013	0.3333
8	50	0.0025	0.007	0.3589
				Average: 0.2342 ± 0.063

According to the data presented in Table 2, the total hypericin content of *Hypericum perforatum* was obtained as 0.2342 ± 0.063 (%). According to the calibration equation ($y = 8 \times 10^{-5}X + 0.001$) with an $r^2 = 0.99$, a linear relationship was achieved between the concentration of hypericin and absorbance at 587 nm.

XRD measurements

X-ray diffractograms were obtained to investigate the changes in the crystalline structure of the pristine electrospun PCL and various PCL-E$_n$ nanofiber membranes. As can be seen from Fig. 3, in all cases two strong diffraction peaks at Bragg angles of 21.4̊ and 23.8̊ were observed, which were attributed to the diffractions of the (110) lattice plane and the (200) lattice plane of semi-crystalline PCL, respectivelyh in accordance with the literature data [38]. Also, the main peak with 2θ equal to 44.4 related to the plant extract was observed in all nanofibrous mats of PCL-E$_n$. The interesting point is that, by observing XRD diffraction samples of PCL loaded with Ex, it is understood that, even in highly concentrated samples (50 %), the basic peak of extract was observed. According to Fig. 3 and the results of crystallinity percent of nanofibrous mats of PCL-E$_n$ in Table 3, it is concluded that the extract is distributed within the PCL fibers. However, in comparison to pure PCL fibers, the peak intensity has been decreased dramatically in other mats. Although by

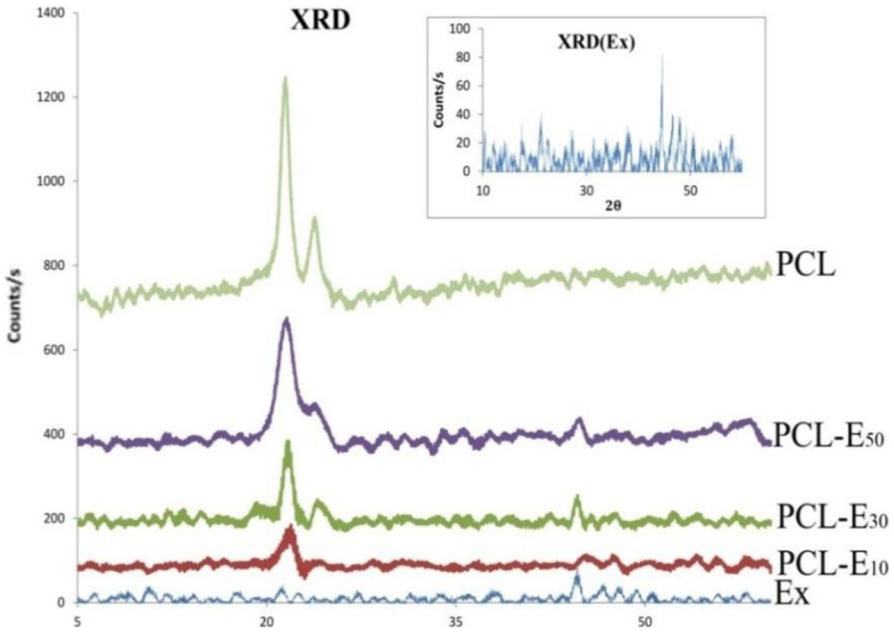

Fig. 3 XRD patterns of pure PCL nanofiber, PCL-E_{50}, PCL-E_{30}, PCL-E_{10} and dried extract. The panel shows the magnified XRD pattern of dried extract

Table 3 Thermal and crystalline properties of electrospun PCL and PCL-E_n nanofiber membranes

Samples	T_m (°C)	ΔH_m (J g^{-1})	X_c (%)
Nanofiber PCL	57.08	71.66	50.46
PCL-E10 nanofiber	48.27	35.03	24.66
PCL-E30 nanofiber	56.71	40.22	28.32
PCL-E50 nanofiber	53.9	45.67	32.16

increasing the content of plant extract, the intensity of diffraction first decreased and then increased. So, according to the above explanations, it is concluded that the interaction of polymer–extract only has an impact on the degree of crystallinity, but the type of PCL crystal nanofibers has not been affected. So, the main peak of PCL occurred at 2θ of 21.4 and 23.8 for all mats and the crystal structure has not changed; just the peak intensity has been changed.

DSC results

Information about the crystallinity of PCL is very useful to correlate with IR spectroscopic results and to verify the attribution of spectral bands. Experimentally, based on the DSC thermograms, we estimated the enthalpy of fusion (ΔH_m) for each PCL and PCL-E_n and, when dividing by the reference enthalpy of totally crystalline PCL ($\Delta H_m^o = 142\text{J g}^{-1}$), the degree of crystallinity (X_c) was obtained. The calculated values of X_c for the samples are reported in Table 3.

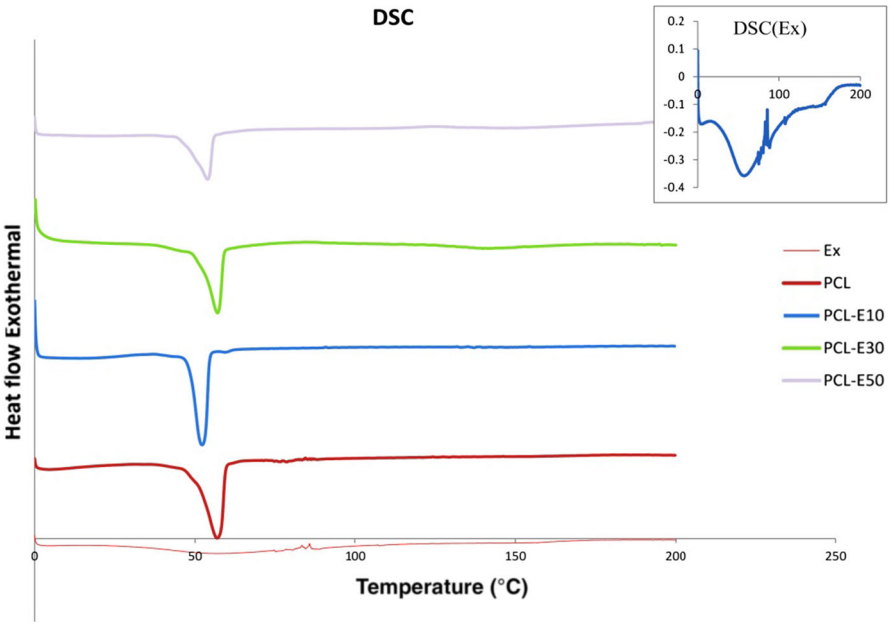

Fig. 4 DSC curves of extract, PCL and PCL-E_n nanofibrous membranes

The DSC curve of the extract shows that a very broad peak is centered at 57.42 °C and for pure PCL exhibited Tm in 57.08 °C (Fig. 4). According to crystallinity calculations, in studying thermal characteristics of PCL-E_n nanofibrous mats (Table 3), the calculated value for crystallinity was obtained as 50.46 % for PCL nanofiber, 24.66 % for PCL-E10, 28.32 % for PCL-E30, and 32.16 % for PCL-E50, which, by comparing the obtained results for PCL-E_n mats Xc, first decreased and then increased.

This is probably because of the reduction in concentration of semi-crystalline PCL in the solution, but the increase in X_c after increasing volumetric percent of extract could be due to polymer–extract interaction.

FT-IR spectroscopy analysis

Incorporation of drug into PCL nanofibers was confirmed by FT-IR spectroscopy and the FT-IR spectra for PCL, herbal drug, and drug-loaded PCL electrospun membranes are shown in Fig. 5.

The peaks at 2942 and 2865 cm^{-1} correspond to asymmetric and symmetric vibrations of the CH group, while C=O vibration of the ester group of the polymer occurs at 1726 cm^{-1}. The peaks at 1107, 1045, and 961 cm^{-1} are due to C=O vibrations with CH_2 rocking vibrations occurring at 732 cm^{-1}. The band at 1294 cm^{-1} is assigned to the backbone C–C and C–O stretching modes in the crystalline PCL. The strong band at 1294 cm^{-1} in the IR spectrum of PCL is its crystallization sensitive peak which is in accordance with the 50.46 % degree of

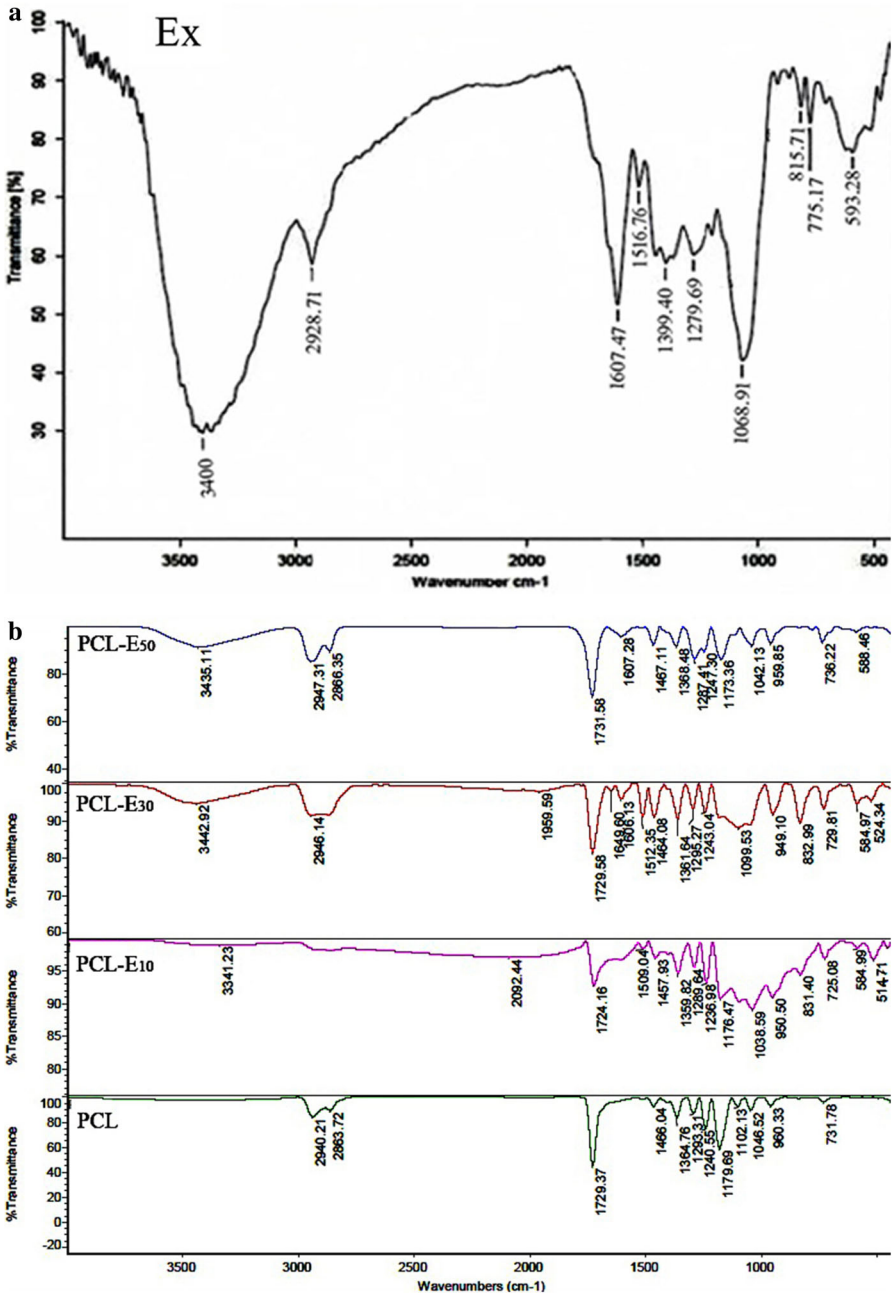

Fig. 5 FTIR spectra of extract, PCL, and PCL-E$_n$ nanofibrous membranes

crystallinity of PCL obtained from the DSC results. Moreover, this band would be useful to investigate the crystallinity changes in PCL thin films after adsorption [39]. Figure 5a displays the FT-IR spectrum of the extract. The peak under

Table 4 Characteristic infrared bands of PCL, extract

Position (cm^{-1})	Vibrator	Abbreviation
2949	Asymmetric CH_2 stretching	υ_{as} (CH_2)
2865	Symmetric CH_2 stretching	υ_S (CH_2)
1727	Carbonyl stretching	υ (C=O)
1293	C–O and C–C stretching in crystalline phase	υ_{Cr}
1240	Asymmetric COC stretching	υ_{as} (COC)
1190	OC–O stretching	υ (OC–O)
1170	Symmetric COC stretching	υ_S (COC)
1157	C–O and C–C stretching in the amorphous phase	υ_{am}
1500–1600	C=C	υ_S (C=C)
880	Rings	The aromatic rings
1200	C–O phenolic	υ (C–O)
3400	OH	υ (O–H)

880 cm^{-1} shows the aromatic rings, C=C stretching appears at 1500 and 1600 cm^{-1} and the peak at 1200 cm^{-1} is related to the C–O phenolic groups. The broad peak at 3400 cm^{-1} is due to the presence of the hydroxyl group's stretching vibrations (Fig. 5a). The FT-IR spectra of the drug-loaded PCL membranes are shown in Fig. 5b. The spectra contain all the features of the peak at 3400 cm^{-1} which is the main evidence for the presence of the extract in the matrix. All the other peaks of the drugs were masked by the vibrations of functional groups in PCL. This confirmed that the drug was present and well associated with the PCL membrane (Table 4).

In vitro drug release

Topical sustained drug delivery is preferred due to the advantages of these delivery systems, such as decreasing the side effects, targeting drug delivery and reducing the frequency of administration. Therefore, it is important to investigate the release profiles. The effective parameters for a transdermally controlled release from electrospun membranes consists of polymer-dependent factors, drug-dependent parameters, carrier system-dependent factors and the biodegradation time of membrane [40]

PCL polymer has very low biodegradation due to its low hydrophilicity. The results of herbal extract release of PCL-E_n nanofiberous mats are shown in Fig. 6. The explosive and very short initial release phase could be due to the drugs trapped near the surface of the fibers. In other words, hydrophobic PCL delayed the penetration of water into the matrix. So, the extract penetration through the amorphous area into the release environment is delayed, which causes a smaller burst release effect.

In the next stage, drug release is slow and the release rate is affected by both the polymer erosion and the drug penetration through the amorphous area of the polymeric matrix. PCL degradation causes slow water diffusion through the polymer, which is the possible mechanism of drug release.

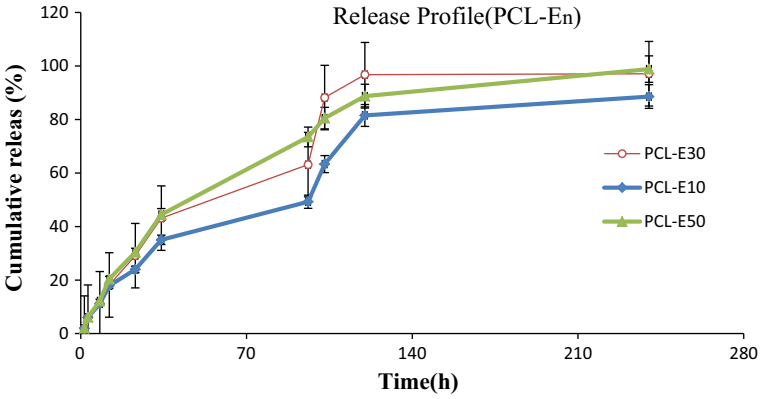

Fig. 6 Cumulative release of hypericin from wound dressings at 37 °C

Furthermore, the polymer degradation rate is very low due to its hydrophobic nature and semi-crystalline structure. Therefore, penetration through the polymeric matrix is the only mechanism of drug release. In other words, when the polymer concentration was decreased, crystallinity was first reduced (from 50.46 to 24.66 %) and then there was an increase in crystallinity due to the polymer–drug interaction despite the reduction in polymer concentration. These results mean that the formed crystalline nanostructures enable a faster release. Due to the coarse crystal structures, the amorphous part becomes broader and the emergence of the large crystalline part leads to faster penetration of the drug through the amorphous part. So, it could be concluded that the internal crystalline structure has a more important role in drug release for the continuous release pattern of nanofibrous mats in comparison to the effect of nanofiber diameter. Although the diameter of the nanofibers affects drug release, because thinner fibers have a better release due to the high surface to volume ratio.

Among nanofibers, PCL-E_{10}, PCL-E_{30} and PCL-E_{50} nanofibrous mats had average diameters of 328 ± 0.067, 412 ± 0.14 and 401 ± 0.01 nm, respectively. In PCL-E_{10}, due to both nanofiber diameter and more amorphous part of polymeric matrix, better burst and continuous release was observed, such that, in 10 % (v/v) of extract, almost 23.95 % release of hypericin was observed in the first 24 h. Then, the release in the next 96 h rose to 49.26 %. In comparison, in the first 24 h, 30.38 % hypericin was released for 30 % (v/v) of extract, while 29.12 % was released for 50 % (v/v) of extract. As is clear from the results of the porosity tests, the scaffold at the concentration of 30 % has more porosity than at the concentrations of 10 and 50 %, which leads to more release of water soluble potassium salt hypericin. Thus, for specific release processes, in cases where drug delivery, depending on the application such as wound healing, must be carried out purposefully, burst release could be considered a positive effect (Fig. 6). It should be noted that, due to hydrophobicity of PCL, penetration is the main mechanism of drug release, in addition to nanofiber diameter, nanofirous mat porosity and nanofibrous mat crystallinity which are effective factors in drug release. So,

regarding the crystallinity of 24.66 % for PCL-E_{10} and the nanofiber diameter of 328 nm for the PCL-E_{10}, the amorphous area of the mat is more than other mats. But PCL-E_{10} nanofibrous mat porosity (91.34 %) is less than PCL-E_{30} porosity (92.85 %). So, since water should penetrate into the pores of the mat, porosity is the main factor in water penetration. The next effective factor is the amorphous area of the hydrophobic polymeric mat, which, according to PCL-E_{10} and PCL-E_{30} crystallinity, this factor along with the porosity factor causes an increase in primary drug release in PCL-E_{30} in spite of a greater PCL-E_{30} nanofiber diameter. Since nanofiber diameter distribution in different volumes of extract does not have a significant effect, the impact of the porosity of the nonwoven mat is more important than the diameter of the nanofibers.

Porosity of nanofibers

Electrospoun membranes with varying percentages of porosity produced a suitable environment for this purpose. The percentage of porosity was 91–92.8 % (Table 1). According to this result, the porosity of the PCL-E_n nanofiber mats prepared here are beneficial for the adherence and proliferation of cells. This slight reduction in the percentage of porosity may be due to the reduction of solvent evaporation after the incorporation of the extract. The reduced solvent evaporation results in higher packing density and thus reducing porosity. Even though there was a reduction in the percentage of porosity, the drug-loaded membranes had very good exudate absorption capability and water vapor transmission rates when compared to the neat PCL.

Results of WVTR

The rate of evaporation of water from the damaged skin must be sufficient to prevent the skin from quick dehydration and yet prevent the accumulation of excessive fluid under the wound covering which facilitates the emergence of infection in the wound. Therefore, the value of this parameter varies in the range of 204 g m^{-2} day^{-1} for a healthy skin, up to 278 g m^{-2} day^{-1} for damaged skin and first-degree burns and 5138 g m^{-2} day^{-1} for a granulating wound. WVTR was measured for three types of dressings and also for a pure PCL nanofiber. In order to simulate a condition in which no dressing is applied to the wound surface, the open surface model was used [23]. The value of WVTR for an effective polymer wound dressing must be in the range of 2000–2500 g m^{-2} day^{-1} [4]. Figure 7 shows the results of WVTR measurements for the membranes. With the incorporation of the extract, the WVTR increased drastically. This may be due to the incorporation of a hydrophilic drug into the membrane. The prepared PCL–E_{50} mats showed a WVTR value of 2675 $\pm$ 30 g m^{-2} day^{-1} due to its lower porosity, thus being close to the adequate range of the ideal wound dressing. Such a WVTR value can strengthen the cellular re-epithelialization.

Pseudo extracellular fluid (PECF) absorption

In order to be used as a high-quality wound dressing, the dressing material should have the ability to absorb excessive exudates from the wound site and keep a

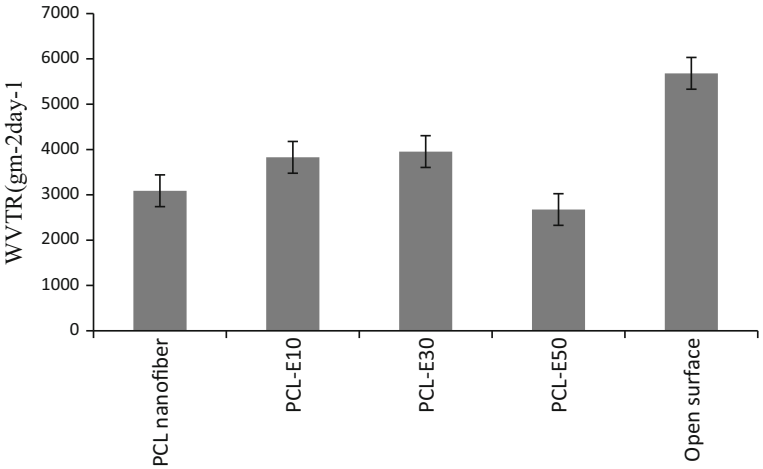

Fig. 7 Results of WVTR for the membranes

suitable moist environment for regeneration of the skin. PECF absorption for the PCL-E_n-loaded membranes was obtained as 71.81, 98.2 and 200 % for PCL-E_{10}, PCL-E_{30} and PCL-E_{50} nanofibrous mats, respectively. It was reported that typical film dressings only show a water absorption of 2.3 % [41], while for polyurethane thick membranes, the water absorption was only 21–26 %. From the results presented in Fig. 8, *Hypericum perforatum* extract-loaded membranes had a better absorption of PECF than the pure PCL nanofibers indicating the better exudate absorption capacity of the drug-loaded membranes (Fig. 8). Because PCL is hydrophobic polymer, increasing the herbal extract of *Hypericum perforatum* in

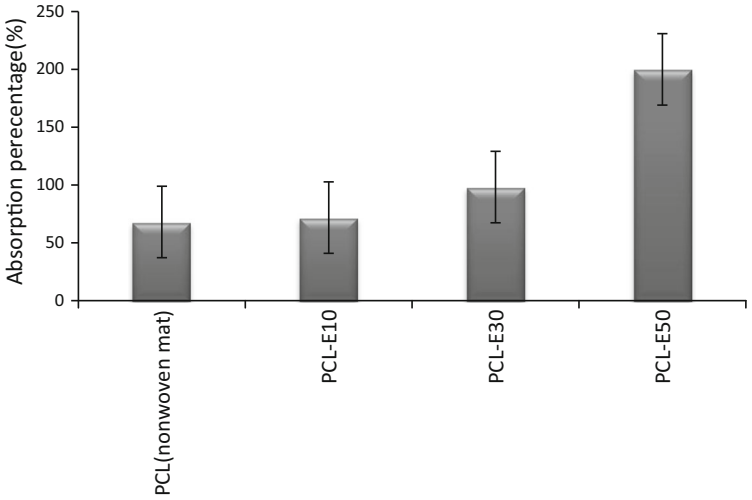

Fig. 8 PECF absorption of the membranes

Table 5 Inhibition zone in mm ± SD of extract at different concentrations in PCL membranes (the results show the average value of three replicates)

Disc diffusion method	*S. aureus* (mm ± SD)	*E. coli* (mm ± SD)
PCL	–	–
PCL-E10	12 ± 0.33	–
PCL-E30	14 ± 0.45	–
PCL-E50	15.66 ± 0.12	–

combination with K_2HPO_4 salt resulted in increasing the hydrophilicity of the polymeric mat. In this research, by adding the alcoholic extract of *Hypericum perforatum*, better absorption for the polymeric mat was observed. Prevention of accumulation of wound exudates is important in the healing of festering wounds, because excessive secretion causes a delay in the cell proliferation process. There is a large variety of wound dressings with varying liquid absorption characteristics available in the literature. In spite of different liquid absorption capacities, each adsorbent can find applications depending on the type of the wound and the amount of secretions. It is also important to prevent the wound from drying out too much.

In vitro antibacterial activities

The inhibitory effect of PCL-E_n against *S. aureus* and *E. coli* was investigated via the disc diffusion method (Table 5). Figure 9 shows the inhibitory zone formation around the nanofibrous discs containing the extract in agar plates of *E. coli* and *S. aureus*. The main reason for this observation was the activity of the *Hypericum perforatum* extract against Gram-positive bacteria with no inhibitory effect on *E. coli* strain. The sample with the wider inhibition zone clearly identified the inhibitory effect of the extract against *S. aureus* compared to the antibacterial activity of the standard antibiogram disc. An increase of the inhibitory zone with increasing the extract concentration can be observed, whereas the extract-loaded specimen gave a 12–16 mm inhibition against *S. aureus* and no inhibition zone against *E. coli*. The explanation can be related to the fact that, in the first 24 h, the quantity of the released *Hypericum perforatum*

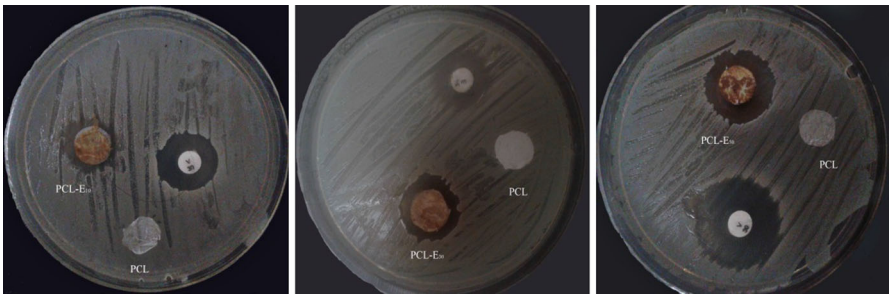

Fig. 9 Inhibitory effects of PCL-E_n against three samples of pathogenic bacteria by means of disc diffusion

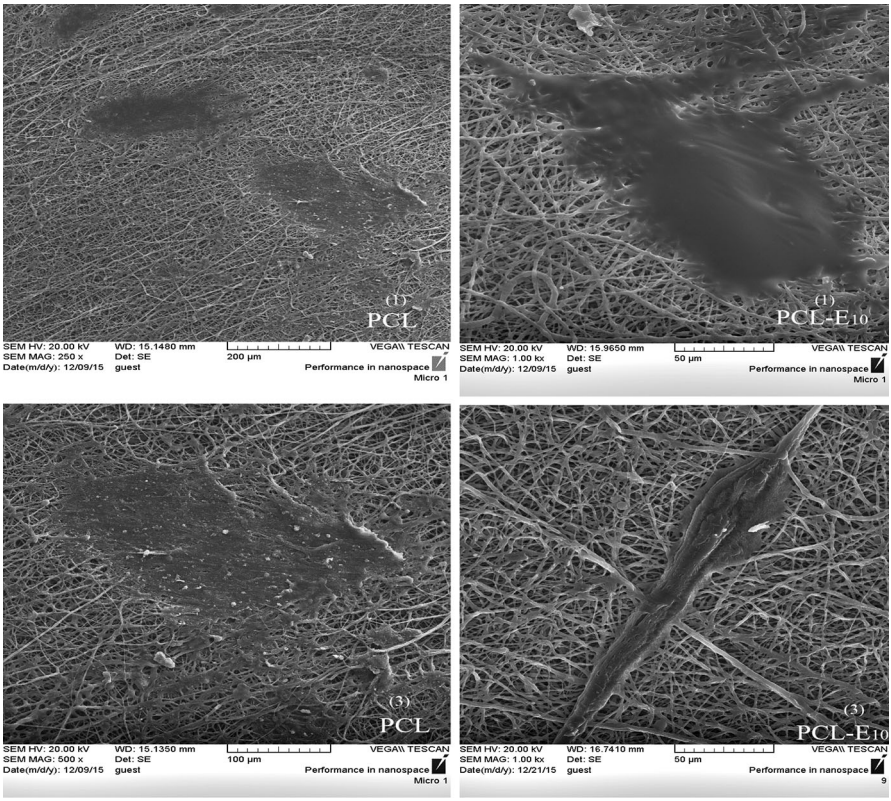

Fig. 10 SEM image of the fibroblast cell on different mats after 1 and 3 days cell culture

extract is not similar in all the samples, so all the samples were checked at 48 and 72 h. The results indicated that the herbal drug-loaded PCL membranes possessed sufficient antibacterial properties to be used as potential wound dressing material.

Cell studies

One of the properties of suitable wound dressings is the ability to induce cells to proliferation and growth. The biologic properties of nanofibrous matrices of neat PCL and PCL-E_{10} were evaluated by using cell culture and biocompatibility tests (MTT assay) in vitro. The results showed that neither tested nanofibrous mats showed any significant toxicity.

In addition to the test data shown in Fig. 10, PCL-E_{10} in cell cultures showed better adhesion after the third day compared to the first day, while in the biocompatibility tests, nanofibrous membranes of neat PCL and PCL-E_{10} had a lower viability percentage of mats on the fifth day compared to the first day, as shown in Fig. 11.

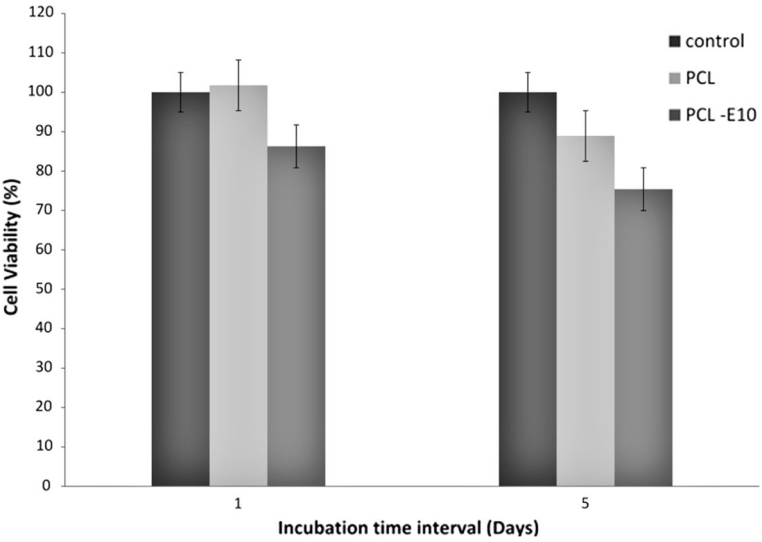

Fig. 11 MTT assay of the attachment and proliferation viability of HSF cell cultured onto PCL, PCL-E_{10}, nanofibrous membranes (1.5 days)

Given that biocompatible pharmaceutical textiles loaded with a herbal drug did not show any significant toxicity, this reduction in the percentage of biocompatibility of neat PCL, and PCL-E_{10} nanofibrous mats could be due to the residual toxic solvents used in manufacturing the nanofibrous memberanes which showed their negative effect on the cells after 5 days of the MTT assay.

However, the viability percentage for extract-loaded PCL membranes was more than 80 %. This confirms that the membranes have good adherance and suitable biocompatibility.

Conclusions

This is the first report on the encapsulation of purified *Hypericum perforatum* extract in PCL by electrospinning. The extract was very rich in flavonoids, mainly quercetin, glucosides and catechins, and exhibited significant antibacterial capacity. The technical parameters for electrospinning PCL, and PCL filled with alcoholic extract at different concentrations of DCM:DMF were defined and set up. A trial-and-error approach has been employed by varying the solution properties and spinning parameters until uniform defect-free fibers were obtained. The morphological analysis showed PCL-E_n fibers with an average diameter of 100–400 nm, whereas the fiber dimensions were slightly increased for samples filled with the extract. The XRD reflections suggested that the *Hypericum perforatum* extract components encapsulated into the PCL fibers are not allowed to crystallize and exist as amorphous molecular aggregates or solid solutions in the fibers. The release properties in the physiological solution show a very short rapid release stage,

followed by a stage in which the release rate is slow, extending for very long time for all the samples. The short stage was analyzed as a function of crystallinity and porosity. In the second stage, the release was found to be very slow, extending up to 240 h for the most concentrated samples.

The antibacterial activity of these electrospun fibers was effective in inhibiting the different proportions of *S. aureus* strain. Human skin fibroblast cells culture on PCL-E_n nanofibrous mats showed that the extract had exceptional properties as a cell growth agent, with increased cell accumulation and was a compatible environment for their viability and proliferation by MTT assay. After the incorporation of the extract, membranes showed no toxic effects to HSF cells. The membranes developed in the present study have great potential in drug delivery and wound healing.

Acknowledgments The authors thank Mr. Mohammad Reza Bastan and his coworkers at Zardband Pharmaceutical Co., Tehran, Iran from their sincere cooperation in carrying out this research and Rasht Branch, Islamic Azad University for their support.

References

1. A. Asif, G. Kakub, S. Mehmood, R. Khunum, M. Gulfraz, Wound healing activity of root extracts of Berberis lyceum Royle in rats. Phytother. Res. **21**, 589–591 (2007)
2. A.A. Hemmati, F. Mohammadian, An investigation into the effects of mucilage of quince seeds on wound healing in rabbit. J. Herbs Spices Med. Plants **7**, 41–46 (2000)
3. A. Seydim, G. Sarikus, Antimicrobial activity of whey protein based edible films incorporated with oregano, rosemary and garlic essential oils. Food Res. Int. **39**, 639–644 (2006)
4. P. Zahedi, I. Rezaeian, S.O. Ranaei-Siadat, S.H. Jafari, P. Supaphol, A review on wound dressings with an emphasis on electrospun nanofibrous polymeric bandages. Polym. Adv. Technol. **21**, 77–95 (2010)
5. L. Smith, P. Ma, Nano-fibrous scaffolds for tissue engineering. Colloids Surf. B **39**, 125–131 (2004)
6. Y. Zhou, D. Yang, X. Chen, Q. Xu, F. Lu, J. Nie, Electrospun water-soluble carboxyethyl chitosan/poly (vinyl alcohol) nanofibrous membrane as potential wound dressing for skin regeneration. Biomacromolecules **9**, 349–354 (2007)
7. H.I. Chang, Y.C. Lau, C. Yan, A. Coombes, Controlled release of an antibiotic, gentamicin sulphate, from gravity spun polycaprolactone fibers. J. Biomed. Mater. Res. Part A **84**, 230–237 (2008)
8. G.D. Mogoşanu, A.M. Grumezescu, Natural and synthetic polymers for wounds and burns dressing. Int. J. Pharm. **463**, 127–136 (2014)
9. G. Jin, M.P. Prabhakaran, D. Kai, S.K. Annamalai, K.D. Arunachalam, S. Ramakrishna, Tissue engineered plant extracts as nanofibrous wound dressing. Biomaterials **34**, 724–734 (2013)
10. D.S. Jones, J. Djokic, C.P. McCoy, S.P. Gorman, Poly (ε-caprolactone) and poly (ε-caprolactone)-polyvinylpyrrolidone–iodine blends as ureteral biomaterials: characterisation of mechanical and surface properties, degradation and resistance to encrustation in vitro. Biomaterials **23**, 4449–4458 (2002)
11. C.G. Pitt, G. Zhong-wei, Modification of the rates of chain cleavage of poly (ε-caprolactone) and related polyesters in the solid state. J. Control. Release **4**, 283–292 (1987)
12. Y. Cha, C. Pitt, The biodegradability of polyester blends. Biomaterials **11**, 108–112 (1990)
13. G. Pitt, M. Gratzl, G. Kimmel, J. Surles, A. Sohindler, Aliphatic polyesters II. The degradation of poly (DL-lactide), poly (ε-caprolactone), and their copolymers in vivo. Biomaterials **2**, 215–220 (1981)
14. Y. Cha, C. Pitt, A one-week subdermal delivery system for L-methadone based on biodegradable microcapsules. J. Control. Release **7**, 69–78 (1988)
15. K.W. Ng, H.N. Achuth, S. Moochhala, T.C. Lim, D.W. Hutmacher, In vivo evaluation of an ultra-thin polycaprolactone film as a wound dressing. J. Biomater. Sci. Polym. Ed. **18**, 925–938 (2007)

16. J.G. Merrell, S.W. McLaughlin, L. Tie, C.T. Laurencin, A.F. Chen, L.S. Nair, Curcumin-loaded poly (ε-caprolactone) nanofibres: diabetic wound dressing with anti-oxidant and anti-inflammatory properties. Clin. Exp. Pharmacol. Physiol. **36**, 1149–1156 (2009)
17. F. Ignatious, J. Baldoni, Electrospun pharmaceutical compositions, in *Google Patents* (2001)
18. P. Opanasopit, U. Ruktanonchai, O. Suwantong, S. Panomsuk, T. Ngawhirunpat, C. Sittisombut, Electrospun poly (vinyl alcohol) fiber mats as carriers for extracts from the fruit hull of mangosteen. J. Cosmet. Sci. **59**, 233–242 (2008)
19. R. Casagrande, S.R. Georgetti, W.A. Verri, M.F. Borin, R.F. Lopez, M.J. Fonseca, In vitro evaluation of quercetin cutaneous absorption from topical formulations and its functional stability by antioxidant activity. Int. J. Pharm. **328**, 183–190 (2007)
20. A. Dias, M. Braga, I. Seabra, P. Ferreira, M. Gil, H. De Sousa, Development of natural-based wound dressings impregnated with bioactive compounds and using supercritical carbon dioxide. Int. J. Pharm. **408**, 9–19 (2011)
21. D. Altiok, E. Altiok, F. Tihminlioglu, Physical, antibacterial and antioxidant properties of chitosan films incorporated with thyme oil for potential wound healing applications. J. Mater. Sci. Mater. Med. **21**, 2227–2236 (2010)
22. S. Rattanakom, P. Yasurin, Chemical profiling of *Centella asiatica* under different extraction solvents and its antibacterial activity, antioxidant activity. Orient. J. Chem. **31**, 2453–2459 (2015)
23. A.G. Namboodiri, R. Parameswaran, Fibro-porous polycaprolactone membrane containing extracts of *Biophytum sensitivum*: a prospective antibacterial wound dressing. J. Appl. Polym. Sci. **129**, 2280–2286 (2013)
24. Z. Karami, I. Rezaeian, P. Zahedi, M. Abdollahi, Preparation and performance evaluations of electrospun poly (ε-caprolactone), poly (lactic acid), and their hybrid (50/50) nanofibrous mats containing thymol as an herbal drug for effective wound healing. J. Appl. Polym. Sci. **129**, 756–766 (2013)
25. L.S. Nair, C.T. Laurencin, Polymers as biomaterials for tissue engineering and controlled drug delivery, in *Tissue Engineering I*, ed. by K. Lee, D. Kaplan (Springer, Berlin, 2006), pp. 47–90
26. R. Upton, *St. John's wort Hypericum perforatum* (American Herbal Pharmacopoeia and Therapeutic Compendium, Scotts Valley, 1997)
27. D. Gîtea, M. Şipoş, T. Mircea, B. Paşca, The analysis of alcoholic extracts of Hypericum species by UV/VIS spectrophotometry
28. Z. Meng, W. Zheng, L. Li, Y. Zheng, Fabrication and characterization of three-dimensional nanofiber membrance of PCL–MWCNTs by electrospinning. Mater. Sci. Eng. C **30**, 1014–1021 (2010)
29. S. Gustaite, J. Kazlauske, J. Bobokalonov, S. Perni, V. Dutschk, J. Liesiene, P. Prokopovich, Characterization of cellulose based sponges for wound dressings. Colloids Surf. A **480**, 336–342 (2015)
30. J.J. Elsner, A. Shefy-Peleg, M. Zilberman, Novel biodegradable composite wound dressings with controlled release of antibiotics: microstructure, mechanical and physical properties. J. Biomed. Mater. Res. B. **93**, 425–435 (2010)
31. S.H. Emami, Z.H. Pirbasti, M.M. Hasani-Sadrabadi, S.S. Kordestani, The effect of isopropanol addition on enhancement of transdermal controlled release of ibuprofen from ethylene vinyl acetate copolymer membranes. J. Appl. Polym. Sci. **122**, 3048–3054 (2011)
32. C.a.L.S. Institute, Clinical and Laboratory Standards Institute, in *Performance Standards for Antimicrobial Disk Susceptibility Tests*, Pennsylvania, USA, 2006
33. L. Boyanova, G. Gergova, R. Nikolov, S. Derejian, E. Lazarova, N. Katsarov, I. Mitov, Z. Krastev, Activity of Bulgarian propolis against 94 *Helicobacter pylori* strains in vitro by agar-well diffusion, agar dilution and disc diffusion methods. J. Med. Microbiol. **54**, 481–483 (2005)
34. J. Kroiss, M. Kaltenpoth, B. Schneider, M.-G. Schwinger, C. Hertweck, R.K. Maddula, E. Strohm, A. Svatoš, Symbiotic streptomycetes provide antibiotic combination prophylaxis for wasp offspring. Nat. Chem. Biol. **6**, 261–263 (2010)
35. G.K. Naughton, J.N. Mansbridge, R.E. Pinney, Culturing fibroblast cells in three-dimensions in a cell culture medium; removing conditioned medium from the cultured cells; combining conditioned medium with a pharmaceutically acceptable carrier, in *Google Patents* (2002)
36. ISO 10993-1 *Biological Evaluation and Biocompatibility Testing of Medical Devices*
37. C.J. Buchko et al., Processing and microstructural characterization of porous biocompatible protein polymer thin films. Polymer **40**(26), 7397–7407 (1999)
38. K. Lee, H. Kim, M. Khil, Y. Ra, D. Lee, Characterization of nano-structured poly (ε-caprolactone) nonwoven mats via electrospinning. Polymer **44**, 1287–1294 (2003)

39. M.M. Coleman, studies of polymer blends containing the poly (hydroxy ether of bisphenol A) and poly (ε-caprolactone). Polymer **24**(3), 251–257 (1983)
40. J.-C. Jeong, J. Lee, K. Cho, Effects of crystalline microstructure on drug release behavior of poly(ε-caprolactone) microspheres. J. Control. Release **92**, 249–258 (2003)
41. T. Li, J. Lin, T. Chen, S. Zhang, Polymeric micelles formed by polypeptide graft copolymer and its mixtures with polypeptide block copolymer. Polymer **47**, 4485–4489 (2006)